JACC: CARDIOVASCULAR IMAGING VOL. 3, NO. 11, 2010

ISSN 1936-878X/$36.00
PUBLISHED BY ELSEVIER INC. DOI:10.1016/j.jcmg.2010.07.014

Increased Pericardial Fat Volume Measured From Noncontrast CT Predicts Myocardial Ischemia by SPECT

Balaji Tamarappoo, PHD, MD,* Damini Dey, PHD,* Haim Shmilovich, MD,* Ryo Nakazato, MD,* Heidi Gransar, MSC,* Victor Y. Cheng, MD,* John D. Friedman, MD,* Sean W. Hayes, MD,* Louise E. J. Thomson, MD,* Piotr J. Slomka, PHD,*† Alan Rozanski, MD,‡ Daniel S. Berman, MD*

Los Angeles, California; and New York, New York

OBJECTIVES We evaluated the association between pericardial fat and myocardial ischemia for risk stratification.

BACKGROUND Pericardial fat volume (PFV) and thoracic fat volume (TFV) measured from noncontrast computed tomography (CT) performed for calculating coronary calcium score (CCS) are associated with increased CCS and risk for major adverse cardiovascular events.

METHODS From a cohort of 1,777 consecutive patients without previously known coronary artery disease (CAD) with noncontrast CT performed within 6 months of single photon emission computed tomography (SPECT), we compared 73 patients with ischemia by SPECT (cases) with 146 patients with normal SPECT (controls) matched by age, gender, CCS category, and symptoms and risk factors for CAD. TFV was automatically measured. Pericardial contours were manually defined within which fat voxels were automatically identified to compute PFV. Computer-assisted visual interpretation of SPECT was performed using standard 17-segment and 5-point score model; perfusion defect was quantified as summed stress score (SSS) and summed rest score (SRS). Ischemia was defined by: SSS − SRS ≥4. Independent relationships of PFV and TFV to ischemia were examined.

RESULTS Cases had higher mean PFV (99.1 ± 42.9 cm^3 vs. 80.1 ± 31.8 cm^3, p = 0.0003) and TFV (196.1 ± 82.7 cm^3 vs. 160.8 ± 72.1 cm^3, p = 0.001) and higher frequencies of PFV >125 cm^3 (22% vs. 8%, p = 0.004) and TFV >200 cm^3 (40% vs. 19%, p = 0.001) than controls. After adjustment for CCS, PFV and TFV remained the strongest predictors of ischemia (odds ratio [OR]: 2.91, 95% confidence interval [CI]: 1.53 to 5.52, p = 0.001 for each doubling of PFV; OR: 2.64, 95% CI: 1.48 to 4.72, p = 0.001 for TFV). Receiver operating characteristic analysis showed that prediction of ischemia, as indicated by receiver-operator characteristic area under the curve, improved significantly when PFV or TFV was added to CCS (0.75 vs. 0.68, p = 0.04 for both).

CONCLUSIONS Pericardial fat was significantly associated with myocardial ischemia in patients without known CAD and may help improve risk assessment. (J Am Coll Cardiol Img 2010;3:1104–12)

From the *Department of Imaging, Cedars-Sinai Medical Center and Cedars-Sinai Heart Institute, Los Angeles, California; †Department of Medicine, David Geffen School of Medicine, University of California Los Angeles, Los Angeles, California; and the ‡Department of Medicine, St. Luke's Roosevelt Hospital, New York, New York. This work was supported by a grant from the National Institute of Biomedical Imaging and Bioengineering (R21EB006829 to Dr. Dey), the Eisner, Glazer, and Lincy Foundations (to Dr. Berman). The authors have reported that they have no relationships to disclose. Drs. Tamarappoo and Dey contributed equally to this work.

Manuscript received May 20, 2010; revised manuscript received July 28, 2010, accepted July 30, 2010.

Pericardial fat volume (PFV) and intrathoracic fat volume (TFV) can be quantified from noncontrast computed tomography (CT) scans performed for coronary calcium scoring (CCS) (1,2). PFV measured on noncontrast CT is strongly associated with coronary artery disease (CAD), CCS, severity of detected CAD, biochemical markers of systemic inflammation, and risk of future adverse cardiovascular events (2–15). However, whether any relationship exists between PFV and myocardial ischemia has not been determined. Recently, to overcome the excessive time and resources needed for quantifying PFV in a large cohort, we used a case-control study to demonstrate a significant association between PFV and major adverse cardiac event (MACE) risk (15). A case-control study design is often used to initially assess the epidemiologic importance of potentially novel disease markers, leading to subsequent prospective research (16–18). We therefore conducted the following case-control study to evaluate whether PFV and TFV obtained from noncontrast CT would provide additive value for identifying patients with increased risk for ischemia in a group of patients with no previous history of CAD.

METHODS

Patient population and CT imaging. Patients were drawn from a cohort of 1,777 consecutive patients without known coronary artery disease enrolled in the EISNER (Early Identification of Subclinical Atherosclerosis Using Non-Invasive Imaging Research) registry at Cedars-Sinai Medical Center, who underwent noncontrast CT for CCS and myocardial perfusion single-photon emission computed tomography (SPECT) within 6 months of each other (15.5 ± 27.3 days between studies). Inclusion criteria for these patients were adults 45 to 80 years of age with intermediate pre-test probability for CAD defined by: 1) man ≥55 years of age or woman ≥65 years of age; or 2) man between 45 and 54 years of age or woman between 55 and 64 years of age with at least 1 traditional CAD risk factor. Patients with unstable angina, history of myocardial infarction, coronary revascularization, cardiomyopathy, peripheral artery disease, or stroke were excluded. In this cohort, there were 73 patients (population "cases" = 73) with inducible ischemia (summed difference score ≥4). We matched each patient with ischemia to 2 same-sex controls using a propensity score. The technique of propensity score–based matching has been widely used to simultaneously control many confounders (19,20). An overall score was first calculated for each patient using a probit model accounting for age, body mass index (BMI), Framingham risk score (FRS), diabetes, clinical symptoms at the time of SPECT, and CCS categories defined as CCS = 0, CCS = 1 to 99, CCS = 100 to 399, and CCS >400) with a widely used STATA software module (StataCorp LP, College Station, Texas) (15,21). Each case was then matched to 2 controls using single nearest-neighbor matching, with no replacement. A total of 219 patients (73 cases and 146 controls) thus comprised the study population. This study was conducted according to guidelines of the Cedars-Sinai Medical Center institutional review board. All patients provided written consent for use of their data.

Noncontrast CT was acquired using an electron-beam (e-Speed, GE Healthcare, Milwaukee, Wisconsin) or a 4-slice CT scanner (Somatom Volumezoom, Siemens Medical Solutions, Forchheim, Germany). Both scanners were calibrated daily using air and water phantoms. Each scan extended from the aortic arch to the diaphragm and was obtained during a single breath-hold. The following scan parameters were used: heart rate dependent, prospective, electrocardiography (ECG) triggering (typically 45% to 60% of the R-R interval), 35-cm field of view, and 512 × 512 matrix size. Tube voltage was 120 kVp with multislice scanning. Slice thickness was 3 mm for electron-beam CT and 2.5 mm for multislice CT.

ABBREVIATIONS AND ACRONYMS

CAD = coronary artery disease
CCS = coronary calcium score
CT = computed tomography
MACE = major adverse cardiac event(s)
PFV = pericardial fat volume
SPECT = single-photon emission computed tomography
TFV = thoracic fat volume

All CT images were reviewed by an expert reader, using semiautomatic commercially available software (ScImage, Los Altos, California) to quantify coronary calcium. Total Agatston CCS was calculated as the sum of calcified plaque scores of all coronary arteries (22). The CT images were transferred to a research workstation for pericardial and thoracic fat quantification.

Pericardial and thoracic fat quantification. Pericardial and thoracic fat quantification was performed by software (QFAT) developed at Cedars-Sinai Medical Center (Los Angeles, California), as previously described (1,15). Pericardial fat was defined as adipose tissue enclosed by the visceral pericardium, including fat directly surrounding the coronary arteries. Thoracic fat was defined as all adipose tissue within the chest at the level of the heart, enclosed by the posterior limit of the heart and above the diaphragm, with the same cranial and

caudal boundaries defined for pericardial fat. Thoracic fat comprised both pericardial and extrapericardial fat.

For defining pericardial contours, the upper slice limit, marked by bifurcation of the pulmonary trunk, and lower slice limit, identified as the slice just below the posterior descending artery, were chosen. This lower limit was chosen to better distinguish pericardial fat from fat around the diaphragm. As in our previous work (1,15), 5 to 7 control points on the pericardium in each transverse view were assigned by an expert reader blinded to patient status and clinical noncontrast CT interpretation. From these control points, piecewise cubic Catmull-Rom spline functions were automatically generated to create a smooth closed pericardial contour (23) for quantification of PFV and TFV (in cm^3). Contiguous 3-dimensional voxels between −190 HU to −30 HU were defined as fat voxels by default (4,24–26); these limits could be modified by the user if deemed appropriate. Figure 1 shows a case example of PFV and TFV measurement.

Exercise and adenosine stress SPECT protocols. Patients were instructed to discontinue beta-blockers and calcium antagonists 48 h and nitrates 24 h before testing. Rest perfusion images were acquired 10 min after infusion of 3 to 4.5 mCi of ^{201}Tl (based on body weight). Stress testing was performed with a symptom-limited Bruce treadmill exercise protocol or vasodilator challenge, as described previously (27). At near-maximal exercise, ^{99m}Tc-sestamibi (32 to 40 mCi) was injected intravenously, after which treadmill exercise was continued at maximal workload for 1 min and at 1 stage lower for 2 additional min whenever possible. ^{99m}Tc-sestamibi myocardial perfusion imaging (MPI) acquisition was started 15 to 30 min after radiopharmaceutical injection. For vasodilator stress, adenosine was infused at 140 μg/kg/min for 5 min; in ambulatory patients, a low-level treadmill exercise was performed during adenosine infusion (28). At the end of the second minute, ^{99m}Tc-sestamibi (32 to 40 mCi) was injected, and myocardial imaging was started approximately 60 min later (29). A 12-lead ECG was monitored continuously during stress testing. Horizontal or downsloping ST-segment depression ≥1 mm or upsloping ≥1.5 mm was considered positive for ischemia.

SPECT acquisition and reconstruction protocols. The SPECT images were acquired with a 2-detector gamma camera (Philips Adac Forte or Vertex, Philips Medical Systems, Cleveland, Ohio, or E-Cam, Siemens Medical Solutions). High-resolution collimators were used, and acquisition consisted of 64 projections over a 180° orbit, with 64 projections at 25 s/projection for supine ^{99m}Tc acquisition followed immediately by 15 s/projection for prone ^{99m}Tc acquisition (30). Rest ^{201}Tl acquisition was performed at 35 s/projection in supine position only. At each of the 64 projection angles, the image data were recorded into 16 equal ECG-gated time bins. No attenuation or scatter correction was applied. After iterative reconstruction (12 iterations) with Butterworth pre-filtering (cutoff 0.66 cycle/pixel for supine ^{99m}Tc, 0.55 cycle/pixel for prone ^{99m}Tc; order 5), short-axis images were automatically generated (31).

Computer-assisted visual quantification of SPECT. Perfusion defect assessment on SPECT-MPI was performed using computer-assisted visual interpretation by an expert reader with the standard 17-segment, 5-point scoring model. The extent and severity of perfusion defect was quantified as summed stress score (SSS) and summed rest score (SRS). The extent and severity of ischemia was given by summed difference score (SDS = SSS − SRS; SDS ≥4 = abnormal) (32,33).

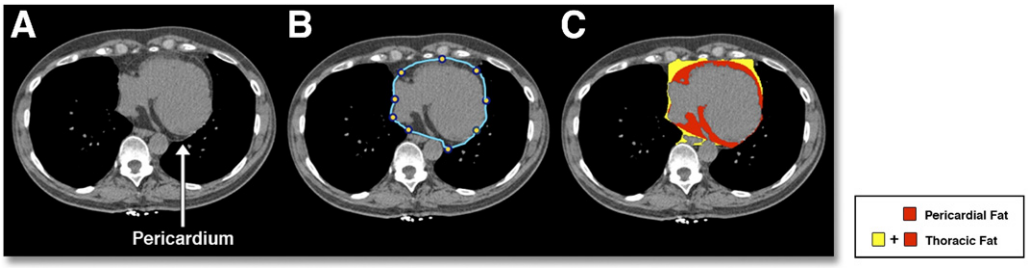

Figure 1. Measurement of PFV and TFV From Noncontrast CT

Pericardial and thoracic fat quantification from a noncontrast computed tomography (CT) for a 65-year-old male patient. **(A)** Shows an axial slice with a clearly visible pericardium. This is manually delineated by the reader **(blue outline)** as shown in **(B)**, and software-based quantification of pericardial and extrapericardial thoracic fat represented by **red and yellow regions**, respectively, is shown in **(C)**. PFV = pericardial fat volume; TFV = thoracic fat volume.

Statistical analysis. Distributions of CCS, PFV, and TFV as continuous variables were non-normal and were thus described as mean ± SD after normalization with logarithmic adjustment. Base-2 logarithmic transformation was chosen because each unit increase represented a doubling of the variable in question (15,34). Other continuous variables were described as mean ± SD. Univariate comparisons between cases and controls were made using the Student *t* test or the chi-square test, as appropriate. Conditional multivariable regression models were generated to evaluate the relationship between PFV, TFV, and CCS with ischemia. Model fit of the conditional logistic regression analyses were checked using the likelihood ratio test to evaluate whether addition of PFV and TFV improved prediction of ischemia. To further examine potential incremental value of PFV and TFV over established risk prediction strategies, receiver-operator characteristic (ROC) curves were constructed and areas under the curve (AUCs) were compared (35). Differences in estimated sensitivity, specificity, and accuracy were compared using the McNemar test. Associations and differences with p values <0.05 were considered significant. All statistical analyses were performed using STATA software (version 10, StataCorp LP).

RESULTS

Our matching technique resulted in no significant differences in age, gender, FRS, and BMI between cases with ischemia and controls without ischemia (Table 1). The distribution of patients among the 4 CCS categories was similar in cases and controls, (chi-square value = 0.76, p = 0.859). Mean log-transformed CCS was slightly increased in cases compared with controls (8.49 ± 3.3 vs. 7.64 ± 3.1, p = 0.06); however, this was not statistically significant. In the overall population, 40% of patients were symptomatic and 60% of patients were asymptomatic. Cases and controls were similar with respect to the proportion of individuals who were symptomatic (angina, dyspnea, atypical chest pain, and dyspnea with angina or atypical chest pain, p = 0.17). By definition, all cases included in our analysis had inducible ischemia, with mean SSS values of 10.5 ± 7.3 and mean SDS values of 9.9 ± 6.8, and none of the controls had inducible ischemia, with mean SSS values of 0.1 ± 0.4 and SDS values of 0.1 ± 0.3.

In 20 patients in this cohort, PFV and TFV were analyzed by 2 independent observers. There was excellent correlation between the 2 observers for PFV and TFV (R = 0.98, p < 0.0001 and R = 0.99, p < 0.0001, respectively). The intraobserver variability was 8.4 ± 5.8% for PFV and 2.4 ± 4.1% for TFV, similar to our previous study with the same software (1,15). Overall, mean PFV was 86.5 ± 36.9 cm^3 and mean TFV was 172.5 ± 77.4 cm^3. The PFV and TFV were highly correlated to each other (r = 0.86, p < 0.0001). Cases had significantly greater mean PFV (99.1 ± 43 cm^3 vs. 80 ± 32 cm^3, p = 0.0003) and TFV (196 ± 83 cm^3 vs. 161 ± 72 cm^3, p = 0.001) than controls. Figure 2 shows an example of a case-control pair. In a univariate analysis, PFV >125 cm^3 and TFV >200 cm^3 were associated with ischemia, and a greater proportion of cases compared with controls had PFV >125 cm^3 (22% vs. 8%, p = 0.004) and TFV >200 cm^3 (40% vs. 19%, p = 0.001). Therefore, we considered 3 equally spaced thresholds about these values (for PFV: 100 cm^3, 125 cm^3, and 150 cm^3; for TFV: 175 cm^3, 200 cm^3, and 225 cm^3). In Table 2, the sensitivity and positive predictive value (PPV) for both PFV and TFV for detection of myocardial ischemia are low, but the specificity and negative predictive value are higher.

Multivariable and ROC analysis. In multivariable analysis that adjusted for age, BMI, presence of symptoms, and traditional risk factors, the only variables that showed a significant association with ischemia were log-transformed CCS, PFV, and TFV (Table 3). The odds ratio (OR) of ischemia for each doubling of PFV was 2.68 (95% confidence

Table 1. Characteristics of Patients Included in Analysis

	Cases (n = 73)	Controls (n = 146)	p Value
Age (yrs)	60.3 ± 10.4	58.9 ± 9.4	0.35
Male	90.4	90.4	1.00
BMI (kg/m^2)	28.1 ± 4.6	27.1 ± 3.8	0.12
Log_2 (CCS)*	8.49 ± 3.3	7.64 ± 3.1	0.06
Framingham risk score	13.34 ± 8.3	11.84 ± 6.9	0.16
Diabetes	10.9	12.3	0.76
Hypertension	70.6	82.2	0.06
Hyperlipidemia	74.7	76.7	0.74
Family history of CAD	28.8	31.5	0.68
Active smoking	14.4	13.7	0.89
Symptomatic	37	46	0.17
CCS categories†			0.86
0–99	8	10	—
100–399	11	13	—
400–999	19	21	—
≥1,000	62	56	—

Values are mean ± SD or %. *Logarithmic transform of CCS was performed to adjust for its non-normal distribution. †Comparison across all CCS categories.
BMI = body mass index; CAD = coronary artery disease, CCS = coronary calcium score.

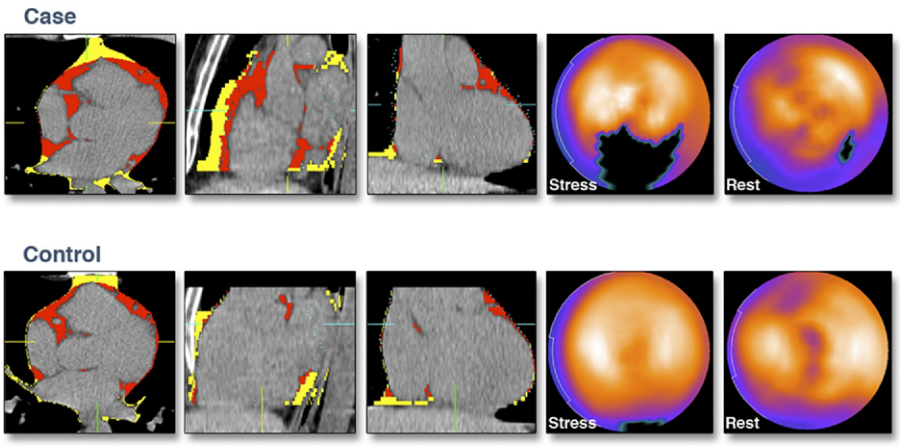

Figure 2. Representative Example of PFV, TFV, and Myocardial Ischemia in a Matched Case-Control Pair

Association of increased pericardial fat and thoracic fat with ischemia. The **top** and **bottom panels** show **(from left to right)** axial, coronal, and sagittal sections of a noncontrast CT with pericardial fat in **red** and thoracic extrapericardial fat in **yellow.** The **last 2 panels on the right** show a polar map of rest and stress myocardial perfusion, with the **darkest region** representing the region of greatest perfusion deficit. The **top panel** represents a patient with ischemia (case) with PFV, TFV, and CCS of 136 cm^3, 227 cm^3, and 150, respectively; the **bottom panel** represents a control patient with PFV, TFV, and CCS of 90 cm^3, 198 cm^3, and 177, respectively. CCS = coronary calcium score; other abbreviations as in Figure 1.

interval [CI]: 1.33 to 5.41, p = 0.006) and for each doubling of CCS was 1.29 (95% CI: 1.08 to 1.57, p = 0.006). In the model with TFV, the OR for ischemia for each doubling of TFV was 2.59 (95% CI: 1.33 to 5.41, p = 0.005) and for each doubling of CCS was 1.33 (95% CI: 1.1 to 1.59, p = 0.003). When adjusting only for CCS, PFV, or TFV, PFV and TFV remained strongly associated with ischemia (OR: 2.91, 95% CI: 1.53 to 5.52, p = 0.001 per doubling of PFV vs. OR: 1.26, 95% CI: 1.05 to 1.51, p = 0.01 per doubling of CCS; OR: 2.64, 95% CI: 1.48 to 4.72, p = 0.005 per doubling of TFV vs. OR: 1.28, 95% CI: 1.08 to 1.53, p = 0.001 per doubling of CCS) (Table 4). The PFV was weakly correlated with CCS (Spearman rho coefficient 0.15, p = 0.02), but TFV was not correlated (Spearman rho 0.12, p = 0.07).

In ROC analysis, when PFV or TFV was incrementally added to CCS, prediction of ischemia by SPECT, as indicated by the ROC AUC, increased significantly from 0.68 to 0.75 (p = 0.04) for PFV and from 0.68 to 0.75 (p = 0.04) for TFV (Figs. 3 and 4). In contrast, association of extrapericardial thoracic fat (defined as: TFV − PFV) with ischemia was much lower (OR: 1.83, 95% CI: 1.18 to 2.84, p = 0.007), with smaller, nonsignificant increases in the ROC AUC (0.68 to 0.72, p = 0.12) when incrementally added to CCS.

DISCUSSION

Our results showed that PFV and TFV measured by noncontrast CT are strongly associated with ischemia by SPECT; to our knowledge, this is the first demonstration of the additive value of PFV and TFV for prediction of ischemia.

It has been suggested that pericardial fat may simply be a marker of overall metabolic risk rather

Table 2. Sensitivity, Specificity, and PPV and NPV for PFV and TFV Thresholds for Detection of Ischemia

Threshold	Sensitivity	Specificity	PPV	NPV	# of Controls	# of Cases
PFV ≥100 cm^3	37.0*	78.8*	46.6	71.4	31	27
PFV ≥125 cm^3	21.9*	91.8*	57.1	70.2	12	16
PFV ≥150 cm^3	12.3*	97.3*	69.2	68.9	4	9
TFV ≥175 cm^3	47.9	68.5*	43.2	72.5	46	35
TFV ≥200 cm^3	41.1	80.8*	51.7	73.3	28	30
TFV ≥225 cm^3	30.1	87.0*	53.7	71.3	19	22

*Significantly different (p < 0.05) across 3 cut points.
NPV = negative predictive value; PFV = pericardial fat volume; PPV = positive predictive value; TFV = thoracic fat volume.

than serving as an active mediator of CAD (4–6,9,10); however, recent studies have shown that increased pericardial fat is strongly associated with increased coronary artery calcium, coronary plaque burden, and MACE. These findings and our observations of the strong association between pericardial fat and ischemia suggest that pericardial fat may play a more direct role in causing coronary atherosclerosis (1,7,8,12–15,38).

Although the exact pathophysiologic mechanism has not been characterized, it has been hypothesized that pericardial fat releases inflammatory signals that promote atherogenesis in coronary arteries (6,12). It is thought that close proximity of pericardial fat to the coronary arteries may play a role in promoting atherogenesis (9,10). In a recent study, Mahabadi et al. (38) showed that there is a strong independent association between the local pericardial (pericoronary) fat that immediately surrounds the coronary arteries and the presence of both noncalcified and calcified coronary artery plaques. More recently Janik et al. (39) showed—in a small cohort of 45 patients—that epicardial fat is associated with ischemia by positron emission tomography and may be a better predictor of ischemia than CCS. The association between increased pericardial fat and ischemia seen in our study may be related to the paracrine effect exerted by pericardial and pericoronary artery fat on coronary atherosclerosis as postulated by Mahabadi et al. (38).

We recently showed that PFV exhibits a significant association with MACE after adjustments for traditional risk factors for CAD and the FRS in a case-control study (15). In a large population-based study, pericardial fat was also found to be strongly associated with a history of adverse cardiovascular events (8). Our observations further highlight the relationship between pericardial fat and CAD by demonstrating that there is a strong association between PFV and myocardial ischemia.

The relative importance of PFV and TFV in mediating coronary atherosclerosis has been a subject of investigation. Rosito et al. (9) showed that PFV but not TFV was associated with coronary calcification. Mahabadi et al. (10) showed that PFV, but not intrathoracic fat (equivalent to the extrapericardial TFV in our study) measured using noncontrast CT, was related to burden of prior cardiovascular disease after adjustment for age, sex, BMI, and waist circumference, suggesting that PFV may be a more specific disease marker. In our analysis, PFV and TFV were dependent variables and increased linearly. Increases in PFV and TFV were both associated with myocardial ischemia. In secondary analysis, the relationship between extrapericardial fat (TFV − PFV) and ischemia was less significant than the association between PFV and ischemia, indicating that the association of TFV is mainly driven by PFV. Our findings suggest that fat stores that immediately surround the coronary artery may have an impact on myocardial ischemia. These findings are consistent with our previous

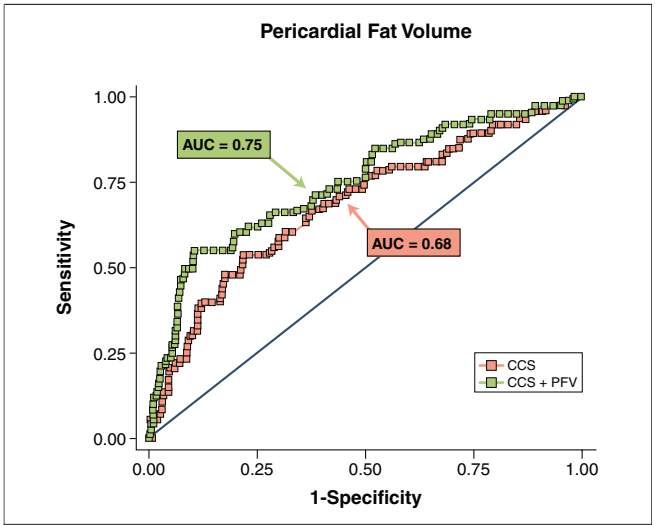

Figure 3. Ischemia Prediction With Addition of PFV

Receiver-operator characteristic curves for prediction of ischemia using logarithmic transform of the CCS alone **(red)** and CCS plus logarithmic transform of PFV **(green)**. AUC = area under the curve; other abbreviations as in Figures 1 and 2.

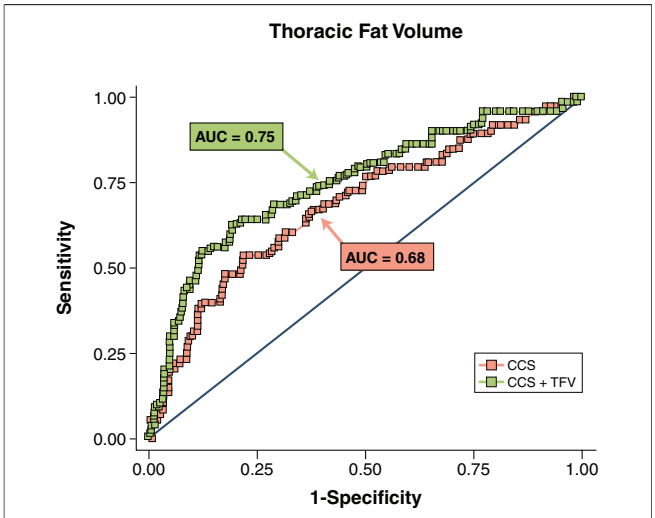

Figure 4. Ischemia Prediction With Addition of TFV

Receiver-operator characteristic curves for prediction of ischemia using logarithmic transform of CCS alone **(red)** and CCS plus logarithmic transform of TFV **(green)**. Abbreviations as in Figures 1, 2, and 3.

Table 3. Conditional Multivariable Regression Analysis Adjusting for BMI, Traditional Risk Factors, Symptoms, CCS, and PFV or TFV

	OR (95% CI)*	p Value
Analysis with PFV		
BMI (kg/m^2)	1.00 (0.93–1.09)	0.86
Log_2 (CCS)†	1.29 (1.08–1.57)	0.006
Diabetes	1.24 (0.44–3.45)	0.68
Hypertension	1.58 (0.71–3.49)	0.26
Hyperlipidemia	1.03 (0.49–2.12)	0.07
Family history of CAD‡	1.36 (0.68–2.68)	0.38
Active smoking	1.19 (0.46–3.08)	0.71
Symptomatic	1.95 (0.96–3.97)	0.06
Log_2 (PFV)†	2.68 (1.33–5.41)	0.006
Analysis with TFV		
BMI (kg/m^2)	1.00 (0.92–1.09)	0.98
Log_2 (CCS)*	1.33 (1.10–1.59)	0.003
Diabetes	1.14 (0.42–3.07)	0.79
Hypertension	1.55 (0.70–3.43)	0.28
Hyperlipidemia	0.96 (0.46–1.98)	0.90
Family history of CAD‡	1.40 (0.71–2.77)	0.33
Active smoking	1.24 (0.49–3.11)	0.65
Symptomatic	1.97 (0.96–3.99)	0.06
Log_2 (TFV)*	2.59 (1.33–5.41)	0.005

*The odds ratio (OR) for ischemia associated with each variable included in the multivariable analysis is given with 95% confidence interval (CI) in parentheses. †Logarithmic transform of CCS, PFV, and TFV was performed to adjust for their non-normal distributions. ‡Family history of premature CAD. Abbreviations as in Tables 1 and 2.

study demonstrating the preferential association between PFV over TFV and risk of MACE (15).

The sensitivity and PPV for both PFV and TFV for detection of myocardial ischemia are low, but the specificity and negative predictive value are higher. The low sensitivity and PPV are expected because this measurement of fat around the coronary arteries is not a direct assessment of the presence of abnormality within the coronary arteries. However, the higher specificity suggests that pericardial fat measurement may potentially help define population subgroups in which further evaluation of myocardial ischemia may be warranted. A CCS ≥400 is traditionally considered to define patients who need further evaluation for ischemia (34,36,37). In patients with metabolic syndrome or diabetes the observed frequency of myocardial ischemia has led to a suggestion that a CCS ≥100 may be a more appropriate threshold (36,40). Our findings suggest that increased PFV may also define a patient group in which a lower threshold for ischemia testing may be appropriate. The significant relationship between pericardial fat and myocardial ischemia in our study needs to be further investigated with additional whole cohort studies.

We have previously shown that a greater number of patients who experienced MACE had a PFV >125 cm^3 compared with event-free controls (15). In this study, we report that a similar threshold of PFV may confer increased risk of myocardial ischemia; an increased proportion of patients with ischemia exhibit PFV >125 cm^3 compared with nonischemic controls.

In our study, patients (cases and controls) were matched based on standard CCS categories (CCS 0 to 99, CCS 100 to 399, CCS 400 to 999, and CCS ≥1,000). Therefore, after matching, the categories were not significantly different ($p = 0.86$); however, log-transformed CCS was not matched, and there is a trend toward significant difference ($p = 0.06$) for log-transformed CCS between cases and controls in univariate analysis. In multivariable analysis, log-transformed CCS was significantly associated with myocardial ischemia. However, because we matched cases and controls based on CCS categories to minimize the confounding effects of CCS, further examination of the relative strengths of CCS and PFV through a whole-cohort study is needed. Our current results lead us to hypothesize that increases in the number of future cardiac events in patients with high PFV and TFV may be related to an increased risk of myocardial ischemia. Whether the risk of ischemia in this patient cohort is related to an increase in coronary plaque burden, stenosis severity, or abnormal endothelial reactivity still remains to be characterized.

Study limitations. A case-control study design, although commonly used to assess the epidemiologic importance of potentially novel disease markers (16,17), is more sensitive to the effects of confounding factors than a cohort study design. We chose a case-control design with rigorous matching of potential confounding variables because complete quantification of both PFV and TFV in a large population using currently available techniques

Table 4. Conditional Multivariable Regression Analysis Adjusting for CCS and PFV or TFV

	OR (95% CI)*	p Value
Analysis with PFV		
Log_2 (CCS)†	1.26 (1.05–1.50)	0.01
Log_2 (PFV)†	2.91 (1.53–5.52)	0.001
Analysis with TFV		
Log_2 (CCS)†	1.28 (1.08–1.53)	0.005
Log_2 (TFV)†	2.64 (1.48–4.72)	0.001

*The OR for ischemia associated with each variable included in the multivariable analysis is given with 95% CI in parentheses. †Logarithmic transform of CCS, PFV, and TFV was performed to adjust for their non-normal distributions. Abbreviations as in Tables 1, 2, and 3.

would be prohibitively time and labor intensive. Our study population consisted of patients without previously known CAD who underwent CCS and MPI by SPECT whether symptomatic or asymptomatic; however, symptoms were matched between cases and controls and were therefore not significantly different (Table 1). Furthermore, PFV and TFV emerged as predictors of ischemia in a multivariable analysis. C-reactive protein was not available for most of our patients, and correlation of C-reactive protein with PFV or ischemia could not be assessed. Our matching for CCS categories minimized the importance of CCS in multivariable analysis. Although our results suggest additive utility of pericardial fat to traditional risk-stratifying factors, including CCS, for prediction of ischemia, confirmation through longitudinal whole-cohort evaluation is needed.

CONCLUSIONS

Pericardial fat was associated with myocardial ischemia in patients without known CAD and may be important for risk stratification.

Acknowledgment

The authors thank Vishal Vashistha for help with data collection.

Reprint requests and correspondence: Dr. Daniel S. Berman, Cedars-Sinai Medical Center, Imaging, 8700 Beverly Boulevard, Taper 1258, Los Angeles, California 90048. *E-mail: bermand@cshs.org.*

REFERENCES

1. Dey D, Wong ND, Tamarappoo BK, et al. Computer-aided non-contrast CT-based quantification of pericardial and thoracic fat and their associations with coronary calcium and metabolic syndrome. Atherosclerosis 2010;209:136–41.
2. Dey D, Suzuki Y, Suzuki S, et al. Automated quantitation of pericardiac fat from noncontrast CT. Invest Radiol 2008;43:145–53.
3. Taguchi R, Takasu J, Itani Y, et al. Pericardial fat accumulation in men as a risk factor for coronary artery disease. Atherosclerosis 2001;157:203–9.
4. Wheeler GL, Shi R, Beck SR, et al. Pericardial and visceral adipose tissues measured volumetrically with computed tomography are highly associated in type 2 diabetic families. Invest Radiol 2005;40:97–101.
5. Fox CS, Massaro JM, Hoffmann U, et al. Abdominal visceral and subcutaneous adipose tissue compartments: association with metabolic risk factors in the Framingham Heart Study. Circulation 2007;116:39–48.
6. Pou KM, Massaro JM, Hoffmann U, et al. Visceral and subcutaneous adipose tissue volumes are cross-sectionally related to markers of inflammation and oxidative stress: the Framingham Heart Study. Circulation 2007;116:1234–41.
7. Ding J, Kritchevsky SB, Harris TB, et al. The association of pericardial fat with calcified coronary plaque. Obesity 2008;16:1914–9.
8. Ding J, Kritchevsky SB, Hsu FC, et al. Association between non-subcutaneous adiposity and calcified coronary plaque: a substudy of the Multi-Ethnic Study of Atherosclerosis. Am J Clin Nutr 2008;88:645–50.
9. Rosito GA, Massaro JM, Hoffmann U, et al. Pericardial fat, visceral abdominal fat, cardiovascular disease risk factors, and vascular calcification in a community-based sample: the Framingham Heart Study. Circulation 2008;117:605–13.
10. Mahabadi AA, Massaro JM, Rosito GA, et al. Association of pericardial fat, intrathoracic fat, and visceral abdominal fat with cardiovascular disease burden: the Framingham Heart Study. Eur Heart J 2009;30:850–6.
11. Sarin S, Wenger C, Marwaha A, et al. Clinical significance of epicardial fat measured using cardiac multislice computed tomography. Am J Cardiol 2008;102:767–71.
12. Mazurek T, Zhang L, Zalewski A, et al. Human epicardial adipose tissue is a source of inflammatory mediators. Circulation 2003;108:2460–6.
13. Greif M, Becker A, von Ziegler F, et al. Pericardial adipose tissue determined by dual source CT is a risk factor for coronary atherosclerosis. Arterioscler Thromb Vasc Biol 2009;29:781–6.
14. Alexopoulos A, McLean DS, Janik M, et al. Epicardial adipose tissue and coronary artery plaque characteristics. Atherosclerosis 2010;210:150–4.
15. Cheng VY, Dey D, Tamarappoo BK, et al. Pericardial fat burden on ECG-gated noncontrast CT in asymptomatic patients who subsequently experience adverse cardiovascular events on 4-year follow-up: a case control study. J Am Coll Cardiol Img 2010;3:352–60.
16. Birjmohun RS, Dallinga-Thie GM, Kuivenhoven JA, et al. Apolipoprotein A-II is inversely associated with risk of future coronary artery disease. Circulation 2007;116:2029–35.
17. Karthikeyan G, Teo KK, Islam S, et al. Lipid profile, plasma apolipoproteins, and risk of a first myocardial infarction among Asians: an analysis from the INTERHEART Study. J Am Coll Cardiol 2009;53:244–53.
18. Albert CM, Nam EG, Rimm EB, et al. Cardiac sodium channel gene variants and sudden cardiac death in women. Circulation 2008;117:16–23.
19. Stukel TA, Fisher ES, Wennberg DE, Alter DA, Gottlieb DJ, Vermeulen MJ. Analysis of observational studies in the presence of treatment selection bias: effects of invasive cardiac management on AMI survival using propensity score and instrumental variable methods. JAMA 2007;297:278–85.
20. D'Agostino RB Jr. Propensity scores in cardiovascular research. Circulation 2007;115:2340–3.
21. Leuven E, Sianesi B. PSMATCH2: Stata module to perform full Mahalanobis and propensity score matching, common support graphing, and covariate imbalance testing, 2003. Available at: http://ideas.repec.org/c/boc/bocode/s432001.html. Accessed September 13, 2010.
22. Agatston AS, Janowitz WR, Hildner FJ, Zusmer NR, Viamonte M Jr, Detrano R. Quantification of coronary artery calcium using ultrafast computed tomography. J Am Coll Cardiol 1990;15:827–32.
23. Catmull E, Rom R. A class of local interpolating splines. Proc Int Conf Comput Aided Geom Des 1974;74:317–26.

24. Yoshizumi T, Nakamura T, Yamane M, et al. Abdominal fat: standardized technique for measurement at CT. Radiology 1999;211:283–6.
25. Kvist H, Chowdhury B, Grangard U, Tylen U, Sjostrom L. Total and visceral adipose-tissue volumes derived from measurements with computed tomography in adult men and women: predictive equations. Am J Clin Nutr 1988;48:1351–61.
26. Sjostrom L, Kvist H, Cederblad A, Tylen U. Determination of total adipose tissue and body fat in women by computed tomography, 40K, and tritium. Am J Physiol 1986;250:E736–45.
27. Berman DS, Abidov A, Kang X, et al. Prognostic validation of a 17-segment score derived from a 20-segment score for myocardial perfusion SPECT interpretation. J Nucl Cardiol 2004;11:414–23.
28. Berman DS, Kang X, Hayes SW, et al. Adenosine myocardial perfusion single-photon emission computed tomography in women compared with men. Impact of diabetes mellitus on incremental prognostic value and effect on patient management. J Am Coll Cardiol 2003;41:1125–33.
29. Hachamovitch R, Hayes SW, Friedman JD, Cohen I, Berman DS. Comparison of the short-term survival benefit associated with revascularization compared with medical therapy in patients with no prior coronary artery disease undergoing stress myocardial perfusion single photon emission computed tomography. Circulation 2003;107:2900–7.
30. Nishina H, Slomka PJ, Abidov A, et al. Combined supine and prone quantitative myocardial perfusion SPECT: method development and clinical validation in patients with no known coronary artery disease. J Nucl Med 2006;47:51–8.
31. Germano G, Kavanagh PB, Su HT, et al. Automatic reorientation of three-dimensional, transaxial myocardial perfusion SPECT images. J Nucl Med 1995;36:1107–14.
32. Slomka PJ, Nishina H, Berman DS, et al. Automated quantification of myocardial perfusion SPECT using simplified normal limits. J Nucl Cardiol 2005;12:66–77.
33. Berman DS, Kang X, Gransar H, et al. Quantitative assessment of myocardial perfusion abnormality on SPECT myocardial perfusion imaging is more reproducible than expert visual analysis. J Nucl Cardiol 2009;16:45–53.
34. Detrano R, Guerci AD, Carr JJ, et al. Coronary calcium as a predictor of coronary events in four racial or ethnic groups. N Engl J Med 2008;358:1336–45.
35. DeLong ER, DeLong DM, Clarke-Pearson DL. Comparing the areas under two or more correlated receiver operating characteristic curves: a nonparametric approach. Biometrics 1988;44:837–45.
36. Rozanski A, Gransar H, Wong N, et al. Use of coronary calcium for predicting inducible myocardial ischemia: influence of patients' clinical presentation. J Nucl Cardiol 2007;14:669–79.
37. Chang SM, Nabi F, Xu J, et al. The coronary artery calcium score and stress myocardial perfusion imaging provide independent and complementary prediction of cardiac risk. J Am Coll Cardiol 2009;54:1872–82.
38. Mahabadi AA, Reinsch N, Lehmann N, et al. Association of pericoronary fat volume with atherosclerotic plaque burden in the underlying coronary artery: a segment analysis. Atherosclerosis 2010;211:195–9.
39. Janik M, Hartlage G, Alexopoulos N, et al. Epicardial adipose tissue volume and coronary artery calcium to predict myocardial ischemia on positron emission tomography-computed tomography studies. J Nucl Cardiol 2010;17:841–7.
40. Wong ND, Rozanski A, Gransar H, et al. Metabolic syndrome and diabetes are associated with an increased likelihood of inducible myocardial ischemia in patients with subclinical atherosclerosis. Diabetes Care 2005;28:1445–50.

Key Words: computed tomography ■ ischemia ■ pericardial fat ■ SPECT ■ thoracic fat.